4

Nanocrystals in Metallic Glasses

Rainer J. Hebert
University of Connecticut
U.S.A

1. Introduction

Nanocrystals are considered as isolated, nanoscale particles in modern science or as grains of nanocrystalline material. The latter material is comprised of nanocrystals that form a 3-dimensional polycrystal made of nanocrystals and grain-boundaries. Historically, however, nanocrystals are firmly rooted in colloid science and for a long time nanocrystals were used unknowingly as components of composite materials. For example, the coloring of glasses with colloidal gold nanocrystals dates back to the Romans (Freestone et al., 2007). In light of the historical use of nanocrystals as components of macroscopic composite materials it is not surprising that modern materials science continues and expands the use of nanocrystals for composite materials. The ever increasing array of nanoscale objects, for example, nanowires, nanofibers, nanobelts, nanopillars, or nanotubes, along with improving synthesis and characterization options offers a broad range of possible macroscopic composites with nano-particle components. The range of applications is no longer limited to functional properties, but includes structural applications. While the nanocrystals are per definition crystalline and thus reveal a periodic arrangement of atoms, the surrounding matrix can be crystalline or amorphous. For metals-based nanocrystals, the modern era of composite research dawned with the discovery of Guinier-Preston zones and remained focused on nanocrystals embedded in crystalline matrices. For ceramic materials, an important application emerged with the dispersion of nanocrystals in amorphous or glassy ceramic matrices. For example, cook tops are widely available today that are made of ceramic glasses containing dispersions of oxide nanocrystals. On the metals side, bulk composite materials comprised of nanocrystals embedded in amorphous metallic matrices are still relatively novel materials by comparison with their ceramic counterparts.

The interest in nanocrystals for metallic glasses has had two related motivations. From a viewpoint of fundamental material science, metallic glasses offer a very convenient approach for studying crystallization reactions. For conventional metals or alloys, solidification occurs almost instantaneously and it is usually only possible to study the completely crystallized phase experimentally but not the process of crystallization. Crystallization of a metallic glass, by comparison, can be induced as a "slow-motion" process that enables detailed experimental studies of the crystallization process. The formation of nanocrystals from metallic glasses thus represents an ideal vehicle to test and validate crystallization theories. The second motivation for studying nanocrystals in metallic glasses is much more practical and concerns improvements in properties. Iron-based metallic glasses were among the earliest metals-based glasses and it was soon discovered that the crystallization of transition-metal nanocrystals

improved the soft-magnetic properties. A number of commercial products based on Fe-nanocrystals dispersed in melt-spun amorphous ribbons emerged from the early crystallization studies. With the emergence of bulk metallic glasses starting about 1992 the interest in the synthesis of nanocrystal/metallic glass composite materials shifted toward a much broader range of applications and in particular toward structural applications. The role of nanocrystals for fundamental crystallization studies and for applications is related, since only an understanding of the nanocrystal formation enables a controlled synthesis and thus controlled improvements in properties.

This chapter addresses mainly the role of nanocrystals for properties of metallic glasses and the synthesis of nanocrystals in metallic glasses. Although differences exist between metallic glasses and amorphous alloys, in this chapter both terms are used synonymously. For a discussion of the differentiation between amorphous alloys and metallic glasses the reader is referred to an overview article on metallic glasses (Greer, 1995).

2. Synthesis of nanocrystals in amorphous matrices

2.1 Thermal synthesis

The research program from which the first non-thin film metallic glass emerged focused on the formation of Cu-Ag non-equilibrium solid solutions (Duwez, 1981). The solid solutions were obtained from rapid quenching experiments, leaving the solidified products in a highly non-equilibrium condition. The key idea behind Duwez' ground-breaking experiments was to prevent atoms from re-arranging from nearly homogeneous liquid solutions into solid clusters with different compositions. The rapid quenching limited the time at which atoms had sufficient mobility for re-arrangements to such a short period that re-arrangements were effectively inhibited. While the re-arrangements into equilibrium configurations were inhibited, the quenched alloys retained a thermodynamic driving force for transitioning into the phases that would have formed at lower cooling rates. This driving force is fundamental for the synthesis of nanocrystals in metallic glasses, since the nanocrystals represent phases with lower free energies. The different modes of crystallization and thus of reducing the metastability of metallic glasses are shown in Fig. 1. Both diagrams show the free energy—usually Gibbs free energy, but other energy functions such as the Helmholtz free energy could be used as well—as a function of composition. In polymorphous crystallization the product phase has the same composition as the parent phase. In Fig. 1 a the amorphous parent phase transforms into a terminal solid solution with the same composition, c_{poly}. The crystallization product does not have to be a solid solution, however, and Fig. 1 b shows a polymorphous transition from the amorphous phase into a compound phase ("Compound I"). A second crystallization mode is primary crystallization. In this mode the amorphous phase transforms into a terminal solid solution and an amorphous phase with a higher solute content than the initial amorphous phase. The compositions of the terminal solid solution, $c_{p,s.s}$, and the new amorphous phase, $c_{p,a.}$, are obtained from a common tangent construction. Several important nanocrystal/metallic glass composite materials are obtained from primary crystallization reactions, for example, Al-based metallic glasses, or Fe-based metallic glasses. In both systems the crystallization products are nearly pure Al and Fe phases, respectively. A third crystallization mode—eutectic crystallization--is highlighted in Fig. 1 b. In this mode the parent amorphous phase crystallizes into two crystalline products with compositions that are again obtained from the common tangent construction.

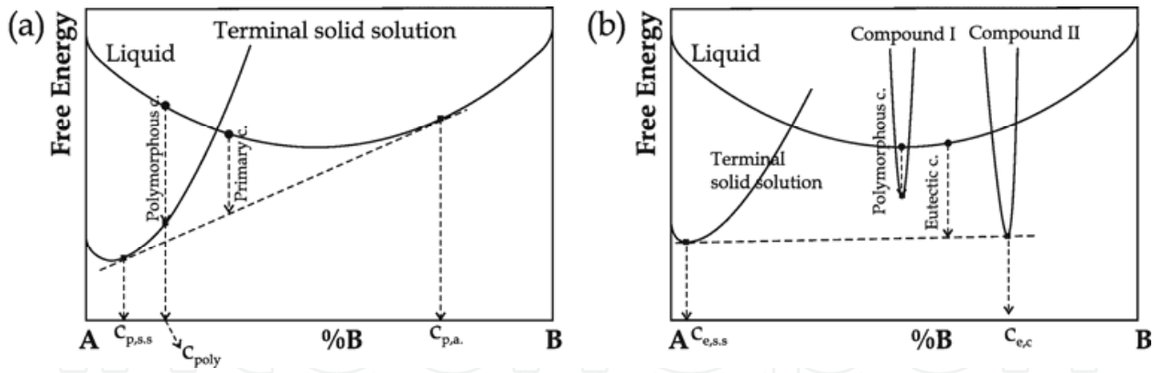

Fig. 1. Free energy curves for hypothetical liquid and solid solution phases vs. composition

Figure 1 shows the different modes of crystallization, but it does not indicate if nanocrystals can be obtained from all crystallization modes. To examine the relation between crystallization mode and the microstructure of the crystallization products, it is necessary to consider the mechanisms of crystallization. Two fundamentally different mechanisms exist: phase separation and nucleation and growth. Both mechanisms are different, but can occur in sequence. For phase separation to occur, the free energy has to reveal a specific composition dependence that is shown schematically in Fig. 2. In composition region II the free energy curve is concave, i.e., $d^2G/dc^2 < 0$. If the initial alloy composition lies within region II any variation in composition lowers the free energy. This scenario is indicated with arrows in Fig. 2. If the initial alloy with composition $c_{initial}$ separates, maybe due to local fluctuations, into two regions with composition c_a and c_b, the mixture of regions with composition c_a and c_b has a lower free energy than the initial region with composition $c_{initial}$. This transition is referred to as spinodal decomposition (Cahn, 1961). If the initial alloy composition lies within regions I and I', however, a small fluctuation in composition will raise the overall free energy. To lower the overall free energy in region I and I', compositional fluctuations have to be finite to lower the free energy.

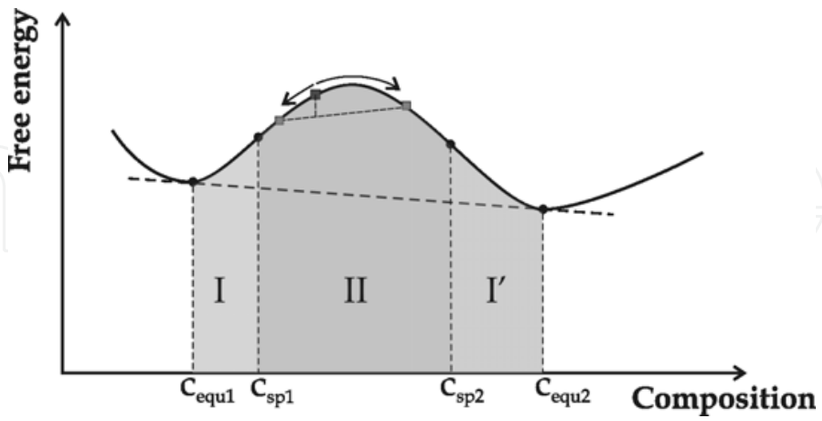

Fig. 2. Free energy vs. composition for a system that reveals spinodal decomposition

In spinodal decomposition transformations an initially single phase separates into two phases with different compositions but the same phase. The composition differences between the compositionally different regions can be minimal, in contrast to nucleation-based phase transformations. In the latter case, thermally induced fluctuations in a parent

phase lead to clusters that are thermodynamically stable once their size exceeds a critical size. Unlike for spinodal decomposition reactions, however, the composition of the new phase is different by a finite amount from the parent phase.

The nucleation and spinodal decomposition theories have been applied successfully for nanocrystal crystallization reactions in metallic glasses. However, several experimental observations suggest that there are open issues related to nucleation or spinodal decomposition reactions that call for continued studies for metallic glasses. For example, several studies on Al-based metallic glasses demonstrated that the addition of minor amounts of some solute atoms—typically on the order of 1 %--can oftentimes dramatically impact the nanocrystal number density, size distribution, and the glass forming ability. The addition of small amounts of V and Ti to $Al_{88}Y_7Fe_5$ metallic glasses induced a tendency for local ordering in the vicinity of the V and Ti atoms, leading to clusters with about 1 nm in size that have a distorted fcc arrangement (Sadoc et al., 2007). These clusters are now recognized as medium-range ordered regions in the metallic glasses (Stratton et al., 2005) that can decisively influence not only the size distribution and particle number density of the nanocrystals (Perepezko et al., 2010) but furthermore the phase formation (Sadoc, Heckmann et al., 2007). The current understanding of microalloying in metallic glasses is very encouraging for designing metallic glasses with specific nanocrystal dispersions. Further work is necessary to understand the formation of inhomogeneities and their effect on the nucleation or phase separation reactions. The classical nucleation theory is based on the notion of random fluctuations in atomic configurations. This notion might have to be modified for atomic configurations that are locally neither fully amorphous nor crystalline.

2.1.1 Growth of crystallites in metallic glasses

Depending on whether partial processes act in a parallel or sequential manner, the fastest (growth mechanism acting parallel) or slowest (sequential) process controls the growth-rate (Kingery et al., 1976). For polymorphic phase transformations the composition of the parent and new phase is identical and long-range diffusion is not necessary. The growth rate of the new phase is limited by the speed at which atoms at the interface between the old and new phase can rearrange from the old to the new phase. This growth mode is referred to as interface-controlled. If the growing particle has a composition different from the matrix, solute diffusion in the matrix is necessary to accommodate the composition change across the phase boundary. In this latter case, one can distinguish between interface and diffusion-controlled growth. Aside from polymorphous transformations where long-range diffusion is not required, interface control is mainly observed for highly anisotropic interfaces and in discontinuous precipitation reactions. Due to the importance of this growth mode it has been treated in several publications (Hillert, 1968; Christian, 1975; Purdy, 1981; Ratke and Vorhees, 2001). For the formation of nanocrystals in metallic glasses, diffusional growth is of particular interest, since the the nanocrystals that have been synthesized in metallic glasses based on thermal processing are often primary nanocrystals and thus require a solute redistribution or diffusion during growth. Among the first and most influential investigations of diffusion-controlled growth is the work by Zener (Zener, 1949) who considered the growth of a spherical particle in a supersaturated matrix of infinite size and a stationary particle/matrix boundary. This growth problem has been treated in detail in two textbooks (Glicksman, 2000; Ratke and Vorhees, 2001).

A more recent example for growth in ternary systems with greatly differing values of the diffusion coefficients is the growth of primary Al in Al-RE-TM systems (RE: rare-earth, TM:

transition metal). For amorphous metallic metal-metal alloys it has been found that the diffusivity correlates with the atomic size of the diffusing species but not necessarily for metal-metalloid amorphous alloys (Sharma and Banerjee, 1989). With respect to the amorphous Al-RE-TM alloys, this observation suggests that the diffusivities of the rare-earth metals in the amorphous matrix should be low compared with the diffusion of the transition-metal atoms. Atom-probe field-ion microscopy (APFIM) experiments were conducted with partially crystalline amorphous Al-Ni-Ce, Al-Ni-Y and Al-Ni-Sm alloys and the concentration profiles of the individual elements were measured. For the amorphous $Al_{87}Ni_{10}Ce_3$ sample the analysis showed that Ce was enriched in a layer surrounding the primary Al nanocrystallites. The thickness of the layer was approximately 3nm (Hono et al., 1995). The Ni atoms did not show any segregation at the nanocrystal/amorphous matrix interface. A similar investigation with amorphous $Al_{88}Ni_8Sm_4$ (Zhang et al., 2002) and $Al_{88}Ni_4Sm_8$ (Gloriant et al., 2001) showed, however, that the Sm concentration at the interface was not enhanced although the size difference between Sm and Ce atoms is practically zero and a similar diffusion behavior in the amorphous matrix would therefore be expected. It must be noted, however, that the ribbons in (Hono, Zhang et al., 1995) were not annealed but were taken from a portion of the ribbons that partially crystalline already after the melt-spinning. The Al-Ni-Sm samples, by contrast, were annealed to induce the nanocrystallization and it was argued that in this latter case metastable equilibrium was established. Aside from the Al-based amorphous alloys, Fe-based systems and their crystallization behavior have also been investigated in detail. Solute accumulation at the interface between bcc-Fe nanocrystals and the amorphous matrix was observed by APFIM for an amorphous $Fe_{90}Zr_7B_3$ alloy after annealing at 723K for 60min (Zhang et al., 1996). In this case Zr atoms piled-up at the interfaces. The blocking effect of the solute rich layer on the growth of the nanocrystals is discussed in (Koester, 1993).

Similar to the situation for nucleation, recent experimental observations suggest that the classical growth theories might not capture the growth scenario for some metallic glasses accurately. The observation of new growth mechanisms seem to be related to the presence of local clusters with semi-crystalline atomic configurations. Liu and coworkers examined the growth process of nanocrystals in a deeply undercooled $Zr_{65}Ni_{25}Ti_{10}$ bulk metallic glass that contained nanoscale clusters with imperfect ordering in the as-cast state. A step-wise growth process was discovered that started with a transition of the clusters into one-dimensional, then two-dimensional, and eventually three-dimensional fcc Zr_2Ni nanocrystals (Liu et al., 2007). The initial semi-crystalline nanoscale clusters developed directly into nanocrystals, but it is not clear if a different growth mechanism would have unfolded at reduced undercooling levels. It is clear, however, that the key to the design of nanocrystal dispersions in metallic glasses is a better understanding of the nanoscale clusters with distorted crystalline atomic arrangements or icosahedral structure, their formation and role for nucleation and growth.

2.2 Mechanical processing – deformation-induced crystallization

The transformation mechanisms for crystallization that are highlighted in 2.1 require thermal motion of atoms to initiate the transformations. Other modes of crystallization have been observed, however, that are not initiated with externally applied heating of metallic glasses. These externally induced crystallization modes include irradiation and deformation of metallic glasses. Recently, evidence was found that nanocrystals developed on surfaces of Zr-based metallic glasses in corrosion (Paillier et. al., 2010) pits as a direct response to corrosion (Paillier

et. al., 2010). Electrochemical interactions with metallic glasses can therefore be added to the list of external driving modes for crystallization. In the following, the experimental evidence for deformation-induced crystallization is surveyed. Mechanisms for external, driven crystallization are then summarized. This section is concluded with a summary of deformation-affected crystallization. In contrast to deformation-induced crystallization, deformation can impact crystallization during heat treatments that follow deformation. From a historical perspective, the impact of rolling or tensile loading on annealing-induced crystallization was studied early on, i.e., starting in the early 1970s. Deformation-induced crystallization was not observed until the early 1990s (Schulz et al., 1990).

2.2.1 Experimental findings for deformation-induced crystallization

The majority of deformation processes to induce crystallization are based on mechanical alloying. In this approach amorphous powder or amorphous ribbon pieces are deformed in ball mills. Containers filled with amorphous powder or pieces are shaken and contain steel or ceramic balls that collide, trapping powder particles or ribbon pieces in between. Examples of crystallization reactions that were induced with milling are highlighted in Table 1. In the examples highlighted in Table 1 the samples were sealed in containers that were filled with argon. Some ball milling experiments were conducted with the container being immersed in liquid nitrogen or other cooling media to maintain the samples at ambient temperatures. It was demonstrated that without cooling the temperature of the milled samples can increase by 60 to 120 K (Koch, 1989). The size of the crystallites was in all cases limited to less than about 20 nm. Indeed, Schulz and coworkers stated in what has been the first report on milling-induced crystallization of metallic glasses that the size of the nanocrystals in their milled $Fe_{78}Si_9B_{13}$ amorphous ribbons was less than 3 nm and that in order to thermally induce nanocrystals at this size the samples would have had to be annealed for months (Schulz et al., 1990). To achieve a high particle number density and a small size of crystallites that develop from a nucleation and growth process it is necessary to limit the growth process but to achieve a high nucleation frequency. With annealing this can only be achieved if the annealing temperature remains low compared to the glass transition range. Under these annealing conditions the time for nanocrystals to develop could be on the order of months as Schulz and coauthors stated. Ball milling, therefore, provides a faster processing route for nanocrystal formation at nanocrystal sizes of less than about 10 nm than standard heat treatments.

The formation of nanocrystals is not limited to ball milling as a deformation technique, but has furthermore been observed during bending of metallic glass samples. The bending experiments have been conducted mostly with melt-spun ribbons, although in one example micrometer-sized simple beams were machined and subsequently deformed in a simple bending mode (Ogura et al., 2001). During bending, large compressive and tensile stresses develop on the surfaces of the bent samples. Nanocrystals were observed to form on the compressive side of bent melt-spun ribbons, but not on the tensile side for bending experiments with Al-based amorphous alloys (Jiang and Atzmon, 2003). Atzmon's and coworker's observation of an asymmetric nanocrystallization process contrasts with bending experiments of Ni-P micro-beams; nanocrystals developed on the tensile side of the bent beam (Ogura, Tarumi et al., 2001). While the ball milling-induced experiments were conducted mostly with Fe-based metallic glasses, the majority of the bending experiments that started with Chen and coworkers' report in Nature (Chen et al., 1994) were conducted with Al-based amorphous melt-spun ribbons. The common thread between the

System	Deformation specific	Reference
Fe78Si9B13, Fe66Co18Si1B15	Milling in SPEX 8000 mill with steel balls, high-energy ball milling, formation of α-Fe(Si) nanocrystals	(Schulz et. al. 1990)
Fe78Si9B13	Cryogenic ball milling; formation of 2 nm Fe-nanocrystals	(Huang et. al. 1995)
Fe78Si9B13	Low-energy ball milling; Fe nanocrystals develop during milling at 250 oC, but not during annealing at the same temperature without milling.	(Xu and Atzmon, 1998)
Al90Fe5Gd5 Al90Fe5Ce5	Milling in SPEX 8000 with Cr-steel balls; formation of Al nano-crystals.	(He et. al. 1995)
Fe78Si9B13	Cryogenic ball milling, formation of 2-13 nm α-Fe(Si) and Fe2B nanocrystals	(Huang et. al. 1996)
Fe80B20	Formation of a-Fe and Fe3B nanocrystals, followed by formation of Fe2B nanocrystals and disappearance of Fe3B nanocrystals.	(Fan et. al. 1995)
Fe40Ni40P14B6	Nanocrystals develop initially during high-energy ball milling at the surfaces of the amorphous ribbons; at longer annealing times the bulk of the ribbons/powders crystallizes into γ-(Fe,Ni) and $(Fe,Ni)_3(P,B)$	(Fan et. al. 1999)

Table 1. Examples of ball-milling induced crystallization reactions

bending-induced nanocrystallization reactions is the crystallization process only taking place on one side of the bent samples and the tendency of the nanocrystallites to have at least a partial degree of orientation. Table 2 provides a survey of reports for bending-induced crystallization.

System	Deformation specific	Reference
Al90Fe5Gd5 Al87Ni8.7Y4.3 Al90Fe5Ce5 Al85Ni10Ce5	Bending of ribbons through 180° at room temperature; formation of Al nanocrystals , 7-10 nm in size, in shear bands except for the Al85Ni10Ce metallic glass.	(Chen et. al. 1994)
Ni-11.5 wt% P	Bending of micrometer-size cantilever induces Ni nanocrystals at the tension side of the cantileve surface. Nanocrystals had the same orientation.	(Ogura et. al. 2001)
Al90Fe5Gd5	Bending of melt-spun amorphous ribbons through 180° at -40 °C induces nanocrystals on the compressive side but not on the tensile side.	(Jiang et. al. 2003) (Jiang and Atzmon, 2003)

Table 2. Examples of bending-induced crystallization reactions

In addition to ball-milling and bending, cold-rolling and instrumented indentation have been used to induce nanocrystals in metallic glasses. Nanoindentation-induced crystallization was reported for bulk metallic $Zr_{52.5}Cu_{17.9}Ni_{14.6}Al_{10}Ti_5$ glass (Kim et al., 2002). The Zr_2Ni nanocrystallites had a size between 10 and 40 nm. Moreover, the crystallographic orientation of the nanocrystals was not perfectly random. Instrumented indentation studies on a $Al_{90}Fe_5Gd_5$ metallic glass revealed an isotropic arrangement of Al nanocrystals that developed during indentation at 100 nm/s and 10 nm/s (Jiang et. Al., 2003). The average size of the nanocrystals was 6.4 nm for the 100 nm/s indentation rate and 3.8 nm for the

lower rate. The density of the nanocrystals increased toward the bottom of the indent where the strain is the highest. Furthermore the nanocrystal density is higher for the lower indentation rate.
Crystallization reactions were furthermore induced with intense cold rolling and folding of melt-spun amorphous ribbons (Hebert and Perepezko, 2004; Hebert et al., 2004; Hebert et al., 2005; Park et al., 2005; Louzguine-Luzgin and Inoue, 2006; Hebert and Perepezko, 2007). Similarly to the milling- and bending-induced crystallization reactions the size of the nanocrystals was limited to about 15-20 nm. Nanocrystals developed in some metallic glasses during rolling and folding, but for some metallic glass compositions, notably the $Al_{85}Ni_{10}Ce_5$ metallic glass nanocrystals did not develop until the highest strains that could be imparted on the melt-spun ribbons with the rolling and folding approach.

2.2.2 Mechanisms for deformation-induced crystallization

The main challenge in understanding the mechanism of deformation-induced nanocrystal formation in metallic glasses is to discern between thermal and athermal effects. Under the intense deformation modes that have been used to induce nanocrystals it is inevitable that shear bands develop during the deformation process. Proposed mechanisms for deformation-induced crystallization either follow the argument of adiabatic heating in shear bands as source for crystallization or they follow the argument of enhanced kinetics in shear bands due to the dilatation of the metallic glass in shear bands. Several studies focused on estimates or experimental analyses of the transient temperatures that develop during the shear band formation and propagation (Lewandowski and Greer, 2006; Hongwen et al., 2007; Battezzati and Baldissin, 2008; Jiang et al., 2008). The shear strains within shear bands are estimated to be on the order of 100 % (Jiang et al., 2007). Reported temperature rises vary widely between tenths of a degree to on the order of 1,000 K. Indirect evidence for adiabatic heating as a source for deformation-induced crystallization was provided, for example, in Csontos' and Shiflet's work (Csontos and Shiflet, 1997). Composition profiles were measured around Al nanocrystals of a $Al_{90}Fe_5Gd_5$ metallic glass that was deformed at room temperature and annealed in a separate experiment. The composition profiles for both processing routes were practically identical, suggesting a heating effect as the same source for crystallization in both cases. Further indirect evidence for shear band-related heating as the mechanism for deformation-induced crystallization was obtained in Kim and coworkers' study (Kim et al., 2006). The high-temperature Laves phase that formed in the shear bands during room temperature cold rolling was identical with the Laves phase that formed in the same $Ti_{40}Zr_{29}Cu_9Ni_8Be_{14}$ metallic glass upon annealing. On the other hand, evidence was put forth that the deformation-induced crystallization could not be the result of only adiabatic heating. Shear bands formed on the compressive and the tensile sides of bent Al-based metallic glasses, but nanocrystals developed only on one side. With adiabatic heating as the source and mechanism for crystallization, nanocrystals should develop on both sides bar any major differences in the shear bands between the tensile and compressive sides. Observations of a partial to complete ordering of the deformation-induced nanocrystals (Ogura, Tarumi et al., 2001) are difficult to rationalize based only on a heating argument. With arguments for both sides it seems that the deformation-induced crystallization reactions have both a thermal and a deformation component. Deformation-induced crystallization was more recently observed during uniaxial compression of bulk $Cu_{50}Zr_{43}Al_7$ metallic glass at room temperature (Lee et al., 2006). Lee and coworkers suggested that the

hydrostatic stress component lowered the energy barrier for nucleation while the shear stress component lowered the energy barrier for diffusion (Lee, Huh et al., 2006).

2.3 Mechanical processing – deformation prior and during thermally induced crystallization

Crystallization reactions can occur during deformation at room temperature as described in 2.2, but historically the first relation between deformation and crystallization was established for cold-rolling of melt-spun glassy ribbons followed by annealing. Since then the sequence of deformation and annealing has been studied not only for cold-rolling but furthermore for uniaxial compression. A third group of experiments included deformation during annealing. In this set of experiments the stress state can be selected; hydrostatic and uniaxial stress states were examined for their effect on thermally induced crystallization.

2.3.1 Deformation followed by thermally induced crystallization

The effect of cold-rolling on the crystallization behavior was studied starting in the 1970s, but initially the rolling experiments were coupled with annealing treatments after the cold-rolling (Masumoto and Maddin, 1975; Luborsky et al., 1976; Calvayrac et al., 1980; Noskova et al., 1989; Jin et al., 2001). These studies examined the effects that the cold-rolling had on the thermally induced crystallization process. Masumoto and Maddin determined that during the cold-rolling the atomic arrangement in the $Pd_{80}Si_{20}$ glass became more disordered with the formation of additional irregularities. The crystallization temperature increased with rolling deformation (Masumoto and Maddin, 1975). Luborsky and coworkers cold-rolled $Fe_{40}Ni_{40}P_{14}$ metallic glass ribbons at the same reduction levels than Masumoto of 40 % thickness reduction. Small-angle X-ray scattering experiments indicated the disappearance of scattering centers and thus an increase in randomness with rolling (Luborsky, Walter et al., 1976). Kulik and Matyja compressed stacks of $Pd_{100-x}Si_x$ metallic glass ribbons and observed that the crystallization temperature decreased for the compressed ribbons. The amount of compression was comparable to the roll reduction in Masumoto's and Luborsky's work. Moreover, the decrease in crystallization temperature with compression was a function of composition and with a higher Si content the difference between the crystallization temperatures of deformed and undeformed samples increased (Kulik and Matyja, 1980). Calvayrac and coworkers cold-rolled $Cu_{60}Zr_{40}$ metallic glass ribbons and found a less topologically defined atomic arrangement after cold-rolling. Changes in the crystallization behavior were not found, however (Calvayrac, Harmelin et al., 1980). Noskova and coworkers examined the effect of cold-rolling on the phase formation of $Fe_{81}Si_7B_{12}$ metallic glass ribbons. The main finding was an increase in the number density and a reduction in size of the nanocrystals during the initial primary crystallization reactions following cold-rolling (Noskova, Vil'danova et al., 1989). These results can be compared to the more recent findings of cold-rolling induced nanocrystal formation at room temperature. At rolling reductions of about 40 % a more disordered state seems to be achieved according to Masumoto's, Luborsky's, and Kulik's work. With further cold-rolling, however, nanocrystals develop in shear bands and thus at least locally the level of ordering increases at higher deformation levels. Several questions remain open, however: without doubt, shear bands develop at rolling reductions of 40 %. The Pd-based and Fe-based alloys with about 80 at % metal content and about 20 % metalloid content seem to be "inert" to crystallization during deformation while the primary-crystallizing Al-based metallic glasses reveal deformation-induced crystallization. The crystallization behavior of

metallic glasses following deformation is thus strongly composition dependent. Further work is necessary to identify what aspects of the compositional differences are ultimately responsible for the differences in the response to deformation.

2.3.2 Deformation superposed on thermally induced annealing

Hydrostatic and uniaxial tensile stresses were superposed on thermally induced annealing. The impact of hydrostatic stress conditions on crystallization has been considered in several studies for melt-spun amorphous ribbons and bulk metallic glasses. Emmens and coworkers examined the crystallization behavior of $Pd_{75}Ag_5Si_{20}$ metallic glass under a hydrostatic stress of 600 MPa and observed a shift of the crystallization onset temperatures to higher temperatures (Emmens et al., 1975). They argued that an increase in hydrostatic pressure enhanced the nucleation rate due to a higher density of the crystallizing phase. At the same time, the growth rate was inhibited due to a reduced mobility under hydrostatic pressure (Emmens, Vrijen et al., 1975). Iwasaki and Masumoto examined the crystallization behavior of melt-spun $Pd_{80}Si_{20}$ metallic glass at a hydrostatic pressure of 10,000 MPa (Iwasaki and Masumoto, 1978). Their results indicated that the hydrostatic pressure retarded crystallization over the entire temperature range of crystallization. Iwasaki and Masumoto pointed out that the hydrostatic stress limited the mobility of atoms and thus reduced diffusion-controlled growth. Ye and Lu examined the primary crystallization of $Al_{89}La_6Ni_5$ metallic glass under hydrostatic pressure and found a lowering of the crystallization onset temperature under hydrostatic pressure (Ye and Lu, 1999). The thermodynamic argument based on a higher driving force for crystallization under hydrostatic pressure was tested with nanoindentation-based crystallization at different loading rates (Jiang et al., 2003). The indentation-induced nanocrystals were larger for the higher loading rate than for the lower rate. Jiang and coworkers argued that with the same hydrostatic stress surrounding the indent for both loading rates the slower rate exposes the metallic glass for a longer time to the hydrostatic pressure. Since the slower rate and therefore longer pressure exposure resulted in smaller nanocrystals than for the higher loading rate, the thermodynamic driving force argument could not hold to explain the effect of hydrostatic pressure on crystallization. It was suggested that pressure effect was predominantly kinetic in nature. The effects of hydrostatic pressure on crystallization were summarized in Suryanarayana's and Inoue's book (Suryanarayana and Inoue, 2011):

- The density increase with crystallization of metallic glasses promotes crystallization under hydrostatic pressure. For polymorphous transformation reactions, diffusion is not required and thus hydrostatic pressure should promote crystallization.
- Hydrostatic pressure reduces atomic mobility due to a decrease in the specific volume. For primary and eutectic crystallization reactions the kinetics of the crystallization process should be impeded.
- Hydrostatic pressure can change the crystallization pathway or the crystallization products.

A similar effort included the application of tensile stresses during thermal crystallization (Maddin and Masumoto, 1972; Patterson and Jones, 1979; Tiwari et al., 1982; Claus and von Heimendahl, 1983). The results of the tensile test experiments suggest that the tensile stress improves the volume diffusion capability and thus promotes crystallization for diffusion-controlled growth cases. For crystallization reactions that are interface controlled the tensile stress does not impact the crystallization behavior (Claus and von Heimendahl, 1983).

2.4 Mechanical processing of metallic glass/crystal composites

The synthesis approaches for metallic glass composites containing crystalline second phases fall in one of two general categories. Crystallites can develop "in-situ", i.e., during annealing of metallic glass precursors or during the quenching of the liquid alloys into glassy metals. This approach is very useful and efficient for the synthesis of metallic glasses containing nanocrystals. In addition to the annealing of metallic glasses and the formation of crystallites directly during quenching, metallic glass/crystal composites can be synthesized "ex-situ". The most important example of ex-situ processing is melt-infiltration (Dandliker et al., 1998). In this approach metallic glass is heated up to the supercooled liquid state and subsequently pushed into a form containing the second phase. The form containing the metallic glass and the second phase is then quenched. The second phases that have been used so far include metals, alloys, and nonmetallic materials. Different shapes have been used including fibers, rods, or particles. A major advantage of the melt-infiltration process is that the volume fraction of the second phase can be raised beyond the thermodynamic limits inherent to thermal processing. On the downside it is very difficult to achieve dispersions of nano-sized second phases without agglomeration of the second phase particles.

3. Properties of nanocrystals in amorphous matrices

Most studies of nanocrystal/metallic glass composites focus on the overall composite properties and the impact of the nanocrystals on the composite properties. From particle-matrix composite studies with crystalline materials it is known that not only the size distribution and particle number densities determine the composite properties, but furthermore the morphology of the particles, the defects that might exist in the particles, and the particle composition. This chapter highlights the current knowledge of defects in nanocrystals that are embedded in metallic glasses, their morphology and composition.

3.1 Defects in nanocrystals

Thermally induced nanocrystals in metallic glasses were initially considered to be defect free. This notion appears to be true for the vast majority of nanocrystals that develop during annealing of amorphous precursor alloys. Most investigations focused on Al-based amorphous alloys (Inoue, 1998; Abrosimova and Aronin, 2002) and revealed a defect free nature of the Al nanocrystals that grow to about 20 nm in size during controlled heat treatment (Abrosimova and Aronin, 2007). Aronin, however, reported in 2001 the presence of twins and dislocations in Al nanocrystals of annealed $Al_{86}Ni_{11}Yb_3$ melt-spun ribbons for a nanocrystal with a size of about 25 nm (Aronin, 2001). Louzguine-Luzgin and Inoue found evidence for dislocations in Al nanocrystals with sizes of less than 7 nm in as-spun $Al_{85}Y_4Ni_5Co_2Pd_4$ amorphous ribbons (Louzguine-Luzgin and Inoue, 2006; Louzguine-Luzgin and Inoue, 2007). The dislocations in Louzguine-Luzgin's work were observed for nanocrystals that impinged on each other due to extremely high particle number densities of 10^{24} m^{-3}. It was suggested that the dislocations developed due to microstrains in the nanocrystals and due to the formation of nanocrystals directly during quenching. The quenching, it was argued, inhibited the annihilation of dislocations due to the limited time at elevated temperatures during the quench process. From the reports of Al nanocrystals that were defect free after annealing and the reports of dislocations in nanocrystals that developed directly during quenching a conclusion could be drawn that defects could only

develop in quenched-in nanocrystals. The situation is more complex, though. For a $(Ni_{70}Mo_{30})_{90}B_{10}$ amorphous alloy, stacking faults were observed for thermally induced nanocrystals and for nanocrystal sizes exceeding about 5 nm (Abrosimova and Aronin, 2007). At smaller sizes, the nanocrystals that were comprised of fcc Ni-Mo solid solutions were defect free. The defect character was observed with high-resolution transmission electron microscopy and inferred from X-ray analysis (Abrosimova and Aronin, 2007). The same authors did not observe defects in fcc Al nanocrystals that developed in Al-Ni-RE (rare earth) melt-spun ribbons. The argument to rationalize the differences between the nanocrystal defect existence in the Ni-based and Al-based amorphous alloys was based on defect energies. Unlike the Al nanocrystals that are nearly pure Al, the Ni nanocrystals contain significant solute content. The alloying changes the electron concentration and thus the stacking fault energy. While the stacking fault energy is higher for Ni than for Al, the Ni-Mo solid solution has a much reduced stacking fault energy that is below the stacking fault energy of Al (Abrosimova and Aronin, 2007). The low stacking fault energy enables the formation of stacking faults. Microstrains due to, for example, differences in the thermal expansion coefficient, provide the necessary impetus for the formation of the stacking faults (Abrosimova and Aronin, 2007). The existence of defects in isolated nanoparticles or nanocrystals that are embedded in a matrix was considered by Gryaznov in light of dislocation concepts such as image forces and annihilation at interfaces (Gryaznov et al., 1991). The predictions obtained from Gryaznov's work did not, however, agree with the experimental observations in Abrosimova's work (Abrosimova and Aronin, 2002).

Nanocrystals that develop during intense deformation reactions at ambient deformation temperatures might be expected to contain defects due to the mechanical deformation underlying their genesis. A very limited number of studies focused on the defect content of deformation-induced nanocrystals. Studies on intensely cold-rolled and folded $Al_{88}Y_7Fe_5$ metallic glasses demonstrated that for nanocrystal sizes of less than about 5-10 nm the primary Al nanocrystals were defect free (Hebert et al., 2006). Some Al nanocrystals, however, clearly revealed the presence of defects as shown in Fig. 3.

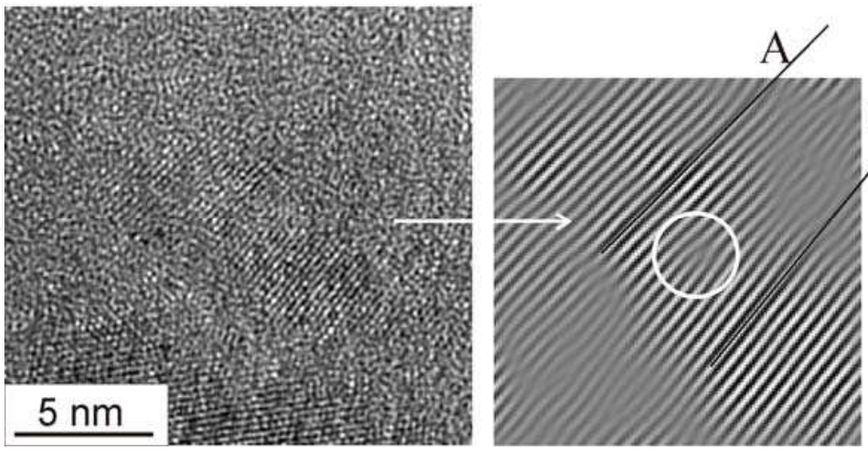

Fig. 3. High-resolution transmission electron microscopy image of an Al nanocrystal in a rolled and folded $Al_{88}Y_7Fe_5$ metallic glass ribbon (left). The Fourier transform (right) reveals the presence of a defect that appears to be a dislocation (Reprinted from (Hebert, Perepezko et al., 2006), with permission from Elsevier)

3.2 Morphology of nanocrystals

Transmission electron microscopy studies have repeatedly shown that nanocrystals developing in amorphous matrices have a spherical shape in the early growth stages, i.e., at a size of about 5-10 nm. An example of a spherical nanocrystal is shown in Fig.4 a.

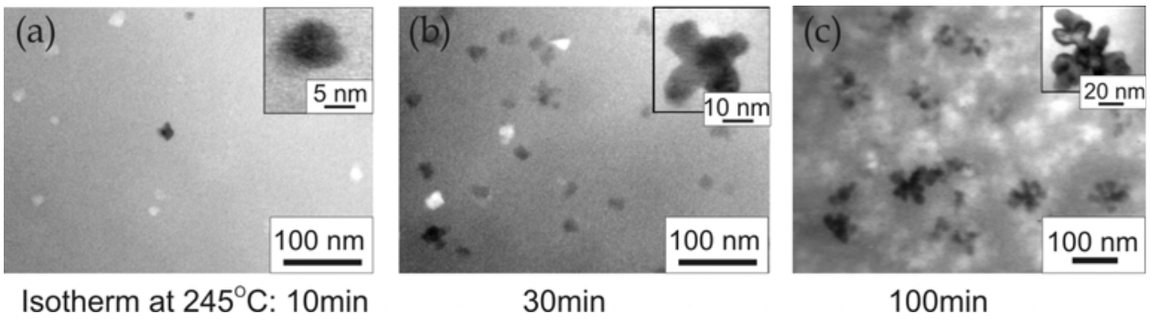

Fig. 4. Bright-field TEM images of $Al_{88}Y_7Fe_5$ melt-spun metallic glass ribbon. (a) after annealing at 245 °C for 10 min. (b) after annealing at 245 °C for 30 min. (c) at 245 °C for 100 min (adapted from (Perepezko and Hebert, 2002)).

The spherical shape of nanocrystals breaks down during further growth. For Al nanocrystals in amorphous Al-based alloys, a dendritic morphology started to develop at sizes of about 10-50 nm as shown in Fig. 4b. While the spherical shape of the nanocrystals during their early growth stage might be expected based on the largely isotropic nature of the metallic glass precursor, recent studies based on molecular-dynamics simulations and high-resolution electron microscopy suggest a morphology of the nanocrystals during the nucleation stage that deviates from the spherical symmetry. The step-wise growth process from one-dimensional ordered arrays into two- and three-dimensional nanocrystals for Zr-Ni-Fi metallic glasses is one example (Liu, Chen et al., 2007).

The transition of the nanocrystals from spherical to dendritic shape might be explained as interface instability. Mullins and Sekerka (Mullins and Sekerka, 1963) investigated the stability of infinitesimal undulations at the interface between a growing particle and the surrounding matrix under the condition that the concentration field can be calculated from the solution of the Laplace-equation. The velocity of each interface element can then be obtained from the mass-conservation equation:

$$v = \frac{D}{C - c_s}\frac{\partial c}{\partial n} \tag{1}$$

where C is the concentration inside the particle, c_s is the concentration in the matrix at the interface and $\partial c / \partial n$ is the concentration gradient at the interface normal to the interface. In order to "generate" undulations, the following ansatz was used for the description of the particle interface:

$$r(\theta,\varphi) = R + \delta Y_l^m(\theta,\varphi) \tag{2}$$

where R is not a function of the angular variables, Y_l^m are the orthonormal set of eigenfunctions for the solution of the Laplace equation for spherical coordinates (spherical harmonics) and δ is the amplitude of the spherical harmonics that is sufficiently small for

higher order terms in δ ($\cong \delta^2, \delta^3, \ldots$) to be negligible. Mullins and Sekerka also included the capillarity effect on the concentration outside the particle at the interface. As a result, an expression for $\dot{\delta}_l$ was obtained, i.e. the change in time of the amplitudes of all spherical harmonic functions. Since this expression is a difference between a concentration gradient term (> 0) and a capillarity term (< 0), the amplitudes can grow (interface becoming unstable) or decay, depending on the relative magnitude of both terms. A key result in (Mullins and Sekerka, 1963) is that the critical size that marks the onset of instability for any of the spherical harmonics is 7R*, with R* the critical size for nucleation. The result for the stability analysis are illustrated schematically in Fig. 5 which is taken from Mullins and Sekerka's seminal paper on interface instability (Mullins and Sekerka, 1963). The solid line denotes the critical size as a function of the parameter - $\frac{c_\infty - c_0}{c_0}$, where c_0 is the concentration of the matrix at the interface for a planar interface (no capillarity effect) and c_∞ the concentration of the matrix at infinity. In the hatched area, the particle is stable, but above the solid line the morphology of the growing particle becomes unstable. The dashed line corresponds to the critical nucleus size. Two trajectories are highlighted that illustrate different growth paths. For an isolated particle in an infinite matrix, the ratio - $\frac{c_\infty - c_0}{c_0}$ is constant therefore the trajectory is vertical. Once the morphology becomes unstable, it continues to be unstable. In case of diffusion-field impingement, c_∞ is time-dependent, therefore the trajectory can be curved. This can lead to the situation depicted in path 2. After an intermediate stage where the particle is unstable it reaches the stable region again.

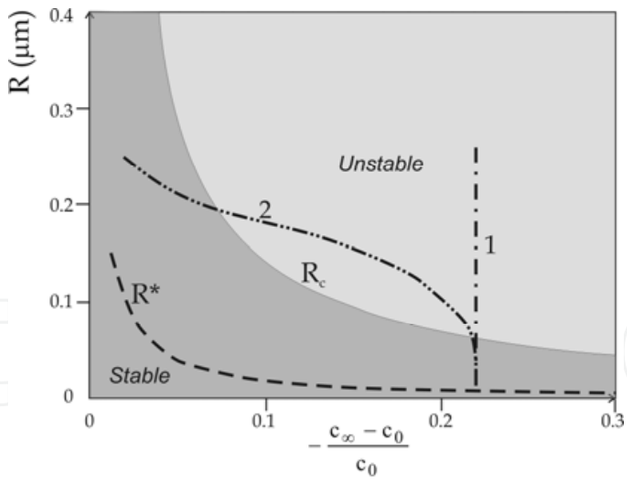

Fig. 5. Critical radius for a spherical particle to become unstable with respect to the spherical shape as a function of the parameter $\frac{c_\infty - c_0}{c_0}$ (adapted from (Mullins and Sekerka, 1963).

The morphology of deformation-induced nanocrystals is not necessarily spherical or dendritic. High-resolution transmission electron microscopy images of Al nanocrystals that developed during intense cold-rolling and folding of metallic glass $Al_{88}Y_7Fe_5$ ribbon revealed prolate shapes of the nanocrystals as shown in Fig. 6. A high-resolution

transmission electron image of an Al nanocrystal in the bent region of a $Al_{90}Fe_5Gd_5$ metallic glass ribbon, however, revealed a nearly spherical shape (Jiang and Atzmon, 2003). Additional insight can be gained from molecular-dynamic simulations. An orientation relationship was observed for the shear- and crystallographic direction of deformation-induced Ni nanocrystals (Tarumi et al., 2000).

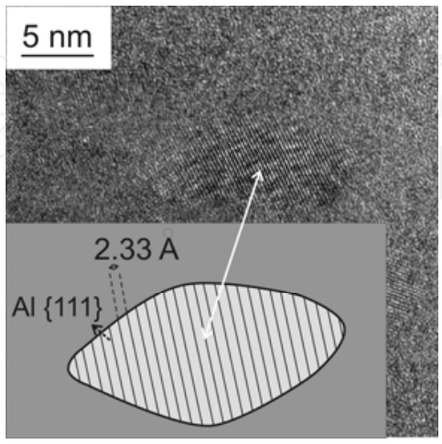

Fig. 6. High resolution transmission electron microscopy image of a Al nanocrystals that developed during repeated cold-rolling and folding of an array of melt-spun $Al_{88}Y_7Fe_5$ metallic glass ribbons (Reprinted from (Hebert, Perepezko et al., 2006), with permission from Elsevier).

4. Effect of nanocrystals on properties of nanocrystal/amorphous composites

4.1 Mechanical properties

Metallic glasses in general offer high strength, elastic resilience (Schuh et al., 2007), and in many cases additional advantageous properties such as high wear resistance (Greer et al., 2002). The substantial differences in the mechanical behavior between crystalline and glassy metals derive from the vastly different deformation mechanisms. Dislocations and stacking faults along with twins are defects that are responsible for the plastic deformation of crystalline materials. At room temperature most metallic glasses deform above a critical stress with the formation and propagation of shear bands. These shear bands are thin—about 20-50 nm—planar regions that deform heavily while the surrounding regions are not or very little affected. During deformation of monolithic metallic glasses a single shear band can propagate throughout the sample and in the process weaken the metallic glass along the shear band to the point of fracture if the deformation is unrestricted (Hays et al., 2000). The Achilles heel of most monolithic metallic glasses for structural applications is thus their limited ductility in tension due to the unrestricted shear band propagation. Many attempts have been made to improve plastic deformation in metallic glasses, including but not limited to specific selections of alloying elements for improved ductility (Gu et al., 2008) or the identification of bulk-glass forming systems that reveal modest plasticity even in the as-cast condition (Schroers and Johnson, 2004). Among the most successful strategies, though, is the dispersion of crystalline particles in amorphous matrices. For micrometer-sized crystalline particles, ductility can be gained but at the expense of a decrease in the overall

composite strength (Bae et al., 2003). Figure 7 a, for example, highlights the dispersion of micrometer-sized brass particles in a warm-extruded $Ni_{59}Zr_{20}Ti_{16}Si_2Sn_3$ metallic glass. While the monolithic glass did not reveal plasticity, a 5 % plastic strain was achieved at 40 vol % brass, but the strength decreased by about 40 %.

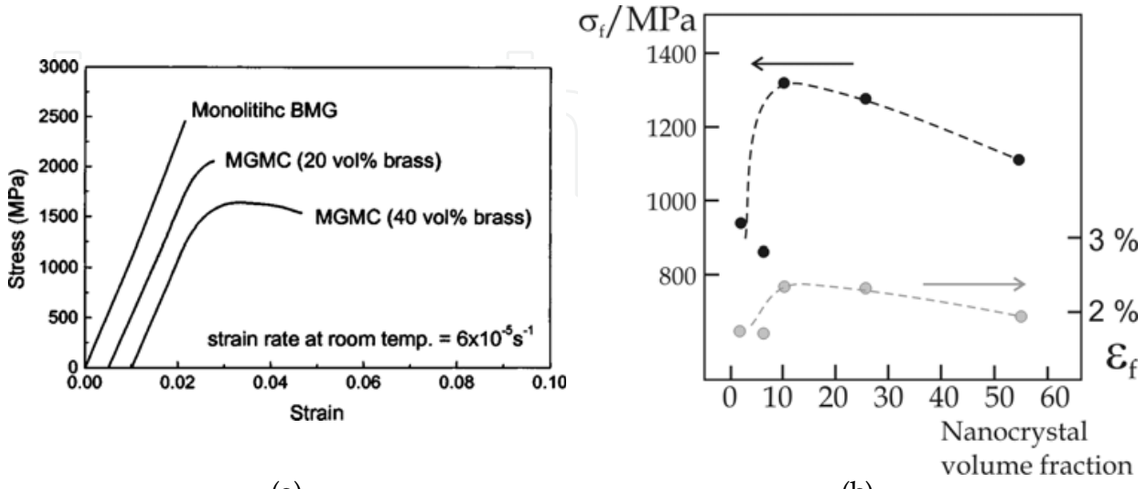

(a) (b)

Fig. 7. (a) The stress vs strain curves of the monolithic sample and MGMCs containing 20 vol % brass and 40 vol % brass tested under the uniaxial compressive condition at room temperature. The load is applied along the extrusion direction (Reprinted with permission from (Bae, Lee et al., 2003). Copyright 2003, American Institute of Physics). (b) Fracture strength σ_f and strain at fracture, e_f, for $Al_{88}Y_2Ni_9Fe_1$ metallic glass as a function of volume fraction of fcc Al nanocrystals (adapted from (Yeong-Hwan et al., 1991)).

Unlike for micrometer-sized crystals in metallic glasses the dispersion of nanocrystals can not only improve the strain to fracture, but can furthermore improve the fracture strength as shown in Fig. 7 b. The dispersion of Al nanocrystals in $Al_{88}Y_2Ni_9Fe_1$ metallic glass raised the fracture stress from about 950 MPa to over 1300 MPa while the strain to fracture increased slightly rather than decreased for a volume fraction of the nanocrystals between 0 and 10 % but decreased at higher volume fractions (Yeong-Hwan, Inoue et al., 1991). The decrease in strain to fracture or ductility with increasing volume fraction of nanocrystals appears to be a general trend (Bian et al., 2002).

Since the deformation behavior of metallic glasses at room temperature and stresses above the elastic limit is tied to the formation and propagation of shear bands, a key topic in understanding the role of nanocrystals and micrometer-sized crystals for the mechanical behavior of metallic glasses is the interaction between shear bands and nano-/micro crystals. This interaction involves not only the role of crystals for interacting with existing and propagating shear bands, but also the role of crystals for the formation of shear bands. It was indeed suggested early on in the development of crystal/metallic glass composites that the role of the crystalline second phase in the amorphous matrices was twofold: first, to serve as initiation or nucleation sites for shear bands and secondly to attract or pin shear bands (Hays, Kim et al., 2000). A parallel between shear bands and their interaction with second phase crystals and dislocations in crystalline materials and their interaction with crystalline second phases is the importance of elastic stress fields. Several studies focused on

the nature of stress fields in the vicinity of crystals and shear bands. Donovan noted (Donovan and Stobbs, 1983) that interactions between shear bands and other sources for elastic stresses in the metallic glasses such as second phase crystals depend on the dilation of the specific volume in shear bands during shear band propagation (Spaepen and Turnbull, 1974; Argon et al., 1985). The dilation of the volume within shear bands induces compressive stresses in the surrounding matrix. The compressive stress field surrounding shear bands would indicate a repulsive interaction with crystals that are surrounded by compressive elastic stress fields and an attraction in case of tensile stress fields. Different sources contribute to elastic stress fields in the vicinity of crystals in metallic glasses. For in-situ formed crystals—either micrometer-sized dendrites or nanocrystals—the annealing induced crystallization reduces the specific volume of the crystalline phase for most metallic glass systems relative to the metallic glass matrix. The stress fields that could develop during the crystallization process, however, are considered to be alleviated due to the elevated temperatures of the metallic glasses during thermally induced crystallization. The elevated temperatures allow the atoms in the surrounding of the crystallites to relax during the crystallization process and therefore potential elastic stresses are relieved. Elastic stresses surrounding crystals furthermore develop during the cooling process from the crystallization process due to the thermal expansion mismatch between crystallites and metallic glasses.

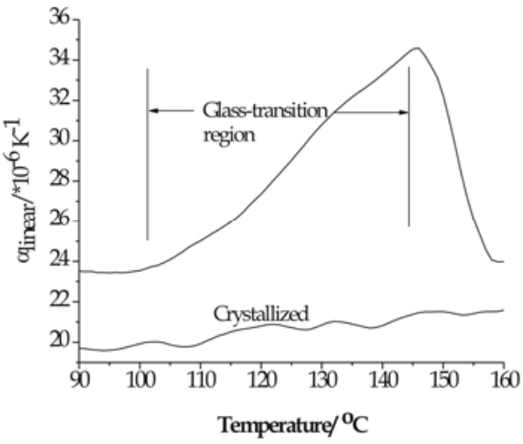

Fig. 8. Thermal expansion coefficient of crystallized and glassy $(Ce_{0.72}Cu_{0.28})_{78.5}Al_{10}Fe_{10}Si_{1.5}$ bulk metallic glass

Figure 8 highlights differences in the true thermal expansion coefficient between a crystallized $(Ce_{0.72}Cu_{0.28})_{78.5}Al_{10}Fe_{10}Si_{1.5}$ metallic glass and the same composition in a glassy state. The temperature range depicted in Fig. 8 includes the glass transition region; the steep drop in the thermal expansion coefficient for the metallic glass sample represents the onset and evolution of crystallization of the metallic glass (Mubarok and Hebert). Upon loading of metallic glasses containing crystals, additional stresses develop due to differences in the elastic and plastic behavior of crystals and glassy matrices. Ott and coworkers examined the stresses in and around micrometer-sized Ta crystals in Zr-Cu-Ni-Ta-Al metallic glasses (Ott et al., 2005). The micrometer-sized Ta crystals were softer than the metallic glass. Plastic

misfit strains developed when the applied load induced plastic strain in the Ta particles while the glassy matrix still deformed elastically. The plastic misfit strains induced localized stress fields in the immediate vicinity of the Ta particles. Shear bands could thus develop in the vicinity of the particles, but could not propagate into the glassy matrix where the stresses remained below the critical stress for yielding. A further important finding in Ott's work (Ott, Sansoz et al., 2005) was that the stress in the glassy matrix was below the applied stress at some matrix locations. The stress fields surrounding the Ta particles were thus highly inhomogeneous and enabled shear band formation and propagation in some areas, but not in other regions until the applied stress increased the stress even in low-stress regions to the point of yielding. As a result, the shear band propagation could not be straight but would be expected to the wavy and possibly deviating from the planes of maximum shear stress. Ott's work was conducted for micro-meter sized crystals and the situation of a soft crystal embedded in a stronger glassy matrix could change for the situation of nanocrystals embedded in glassy matrices. One of the explanations for hardness increases of nanocrystal/metallic glass composites in fact invokes the idea of a hardness increase due to the formation of nanocrystals with hardness levels greater than those of the metallic glass matrices (Yeong-Hwan, Inoue et al., 1991). While the effects of elastic and plastic misfit stresses for the role of shear band propagation have been clearly recognized, further work is necessary to understand in particular the formation of stresses in metallic glasses containing nanocrystals and their effect on shear bands.

4.2 Wear properties

Wear properties of metallic glasses have been studied since 1979 (Boswell, 1979). Until the discovery of bulk metallic glasses, wear studies were conducted on Fe-based and later on Al-based metallic glass melt-spun ribbons (Klinger and Feller, 1983; Miyoshi and Buckley, 1983; Miyoshi and Buckley, 1983; Miyoshi and Buckley, 1984; Kishore et al., 1987; Lim and Ashby, 1987; Gloriant, 2003). Reviews on the wear behavior of melt-spun, ribbon-shaped metallic glasses were prepared by Lim and Ashby (Lim and Ashby, 1987) and Greer, Rutherford, and Hutchings (Greer et al., 2002). The vast majority of studies on the effect of crystallites in metallic glasses on wear properties indicate improvements in the wear behavior with the formation of crystallites. The wear resistance of $Al_{88}Ni_4Sm_8$ metallic glass, for example, increased after an initial phase before reaching a plateau (Gloriant and Greer, 1998). Improvements with partial devitrification of Al nanocrystals were found furthermore for partially crystallized Al-Ni-Y based amorphous alloys (Greer, Rutherford et al., 2002), annealed $Zr_{41}Ti_{14}Cu_{12.5}Ni_{10}Be_{22.5}$ bulk metallic glasses (Li et al., 2002), or partially crystallized bulk $Cu_{50}Hf_{41.5}Al_{8.5}$ metallic glasses (Maddala et al., 2010). The wear improvements at first glance seem to be expected, since the hardness increases in many cases during devitrification. Archard's empirical rule relates hardness directly to wear resistance (Archard, 1957). The hardness, however, continues to increase with further crystallization and often reaches a maximum for the fully crystallized condition (Maddala, Mubarok et al., 2010). The wear resistance does not continue to improve, but often reaches a maximum at a certain degree of crystallization (Boswell, 1979; Vom Wege et al., 1988; Maddala, Mubarok et al., 2010). A possible explanation for the wear changes with crystallization was given early on in Boswell's and Zum Gahr's work (Boswell, 1979; Zum Gahr and Noecker, 1981). With increasing crystallization the hardness increases, but the toughness of the material decreases, i.e., the brittleness of the metallic glass increases. The increasing brittleness of the metallic glass with annealing and crystallization causes a change in the wear mechanism

toward micro-fractures and delamination. Maddala and coworkers have recently confirmed the wear behavior changes with measurements of notch toughness and hardness at different crystallization stages (Maddala and Hebert, 2011).
Several results on the wear behavior of metallic glasses containing nanocrystals, however, seem to contradict the mechanism of a wear improvement with nanocrystal formation and eventual deterioration at higher nanocrystal number densities. Abrasive wear tests on a SiC paper, for example, showed that the wear resistance of the Co-based glass improved with increasing degree of crystallization when fine-grained SiC paper was used (Vom Wege, Skrotzki et al., 1988; Vom Wege et al., 1991). Upon testing with coarse-grained SiC paper, however, the wear resistance deteriorated with increasing crystallinity. The crystallization products were primary Co and Co_3B particles with sizes of 15-20 nm (Vom Wege, Skrotzki et al., 1988). Tam and Shek examined the wear behavior of Cu-Zr-Ti metallic glasses and observed that the hardness did not scale with the wear behavior (Tam and Shek, 2004). Upon closer examination, however, it appears that in Tam's work and Vom Wege's work the wear mechanism was based on micro-fractures. This clearly shows that for wear studies not only the sample need to be considered, but the wear load, condition, atmosphere, amongst others. It seems, however, that under conditions that cause micro-ploughing and micro-cutting the formation of nanocrystals has a positive impact on the wear behavior. Clearly, more work is necessary to identify the relations between the level of crystallization, external wear conditions, and wear behavior.

4.3 Corrosion properties

Metallic glasses in general compare favorably with their crystalline counterparts in their corrosion behavior, although exceptions are known (Hashimoto, 2002; Scully and Lucente, 2005; Scully et al., 2007). The corrosion behavior of single-phase metallic glasses benefits from the lack of structural or chemical inhomogeneities such as grain boundaries or inclusions. It was suggested that metallic glasses promote the formation of amorphous oxides (Scully, Gebert et al., 2007). Many metallic glasses reveal solute levels that far exceed those of their crystalline counterpart systems. The enhanced solute content in the metallic glass can increase the solute content in oxide layers and thus improve the corrosion behavior. The change in interatomic distances and coordination numbers with transition from crystalline to amorphous atomic arrangement furthermore affects electrochemical properties and corrosion properties (Scully, Gebert et al., 2007). Among the earliest corrosion resistance studies on metallic glasses were Fe-metalloid metallic glasses containing chromium. The early studies on Fe-Cr-P-C melt-spun ribbons were continued more recently when bulk metallic Fe-glasses were developed. Bulk metallic glasses in the Fe-Cr-Mo-C-B system revealed corrosion rates as low as 10^{-3} mm/year in concentrated hydrochloric acid.
While the corrosion advantages of fully amorphous metallic glasses are undisputed, the formation of nanocrystals might be expected to negatively impact their corrosion behavior. The nanocrystals, after all, represent both structural and chemical inhomogeneities and entail interfaces with the surrounding amorphous matrices. The chemical inhomogeneities are not limited to the nanocrystal/amorphous matrix interface, but extend into the amorphous matrix due to gradients in solute concentrations that exist at least during the grow stages of nanocrystals that form non-polymorphically. Studies on the corrosion behavior of nanocrystal-containing metallic glasses have been conducted so far for Fe-based,

Ni-based, Zr-based, and Al-based systems. An overall trend, however, does not appear to exist. Even within the same system the corrosion behavior improves for some compositions, but deteriorates for other compositions.

Lucente and Scully examined the corrosion behavior of Al-based amorphous-nanocrystalline alloys containing Al nanocrystals in detail. Four melt-spun amorphous alloys, $Al_{90}Fe_5Gd_5$, $Al_{85}Fe_7Gd_8$, $Al_{90}Co_3Ce_7$, and $Al_{87}Ni_7Gd_6$ were exposed to 0.6 M NaCl electrolyte in an electrolytic cell to test the resistance to micrometer-scale pitting (Lucente and Scully, 2008). The resistance to pitting can be determined quantitatively from measurements of the pitting and repassivation potentials in anodic polarization scans. The pitting potential reflects a resistance to pit initiation and stabilization (Lucente and Scully, 2008). For all four amorphous alloys the repassivation potential remained unchanged when the fully amorphous alloys were partially devitrified. The pitting potential increased compared to the fully amorphous alloy, except for the $Al_{90}Co_3Ce_7$ amorphous alloy that revealed a small decrease in pitting potential with nanocrystal formation. It is noteworthy that the pitting potential increased significantly for the $Al_{85}Fe_7Gd_8$ amorphous alloy despite a nanocrystal size of 100 nm. The increase in pitting potential with nanocrystallization relative to the fully amorphous state suggests that the devitrification inhibits pit initiation. In a second set of experiments, the growth and repassivation kinetics were determined for artificial pits that were induced electrolytically. The growth kinetics of the artificial pits was not affected for the amorphous alloys containing nanocrystals. The unchanged repassivation potential was interpreted as an overall growth kinetics of pits larger than 10 micrometers that were unaffected by the nanocrystal formation.

5. Conclusion

Nanocrystals can significantly improve properties of metallic glasses, for example, mechanical properties or magnetic properties. Some progress has been made to understand the mechanisms behind these improvements, but in many cases a clear understanding has not been achieved, yet. Further work is therefore not only necessary, but promises further advancements. Progress will have to come from a combination of smart experimentation, advanced diagnostics, and computer simulations. Arguably the most interesting aspect of nanocrystals in metallic glasses, though, is the longest-standing issue: their synthesis. Changes in local atomic configuration or changes in nanocrystal number densities by orders of magnitude, or changes in the phase formation with a 1 at % alloying addition offer exciting opportunities to design novel composite materials.

6. References

Abrosimova, G. E., &Aronin, A. S. (2002). The fine structure of FCC nanocrystals in Al- and Ni-based alloys. *Physics of The Solid State*, 44, 6, pp. 1003-1007.

Abrosimova, G. E., &Aronin, A. S. (2007). Size effect on the structure of Al- and Ni-based nanocrystals. *Physics of the Solid State*, 50, 1, pp. 159-163.

Archard, J.F. (1957). Elastic deformation and the laws of friction. *Proc. Roy. Soc. Lond.*, A243, pp. 190-205.

Argon, A. S., Megusar, J., &Grant, N. J. (1985). Shear band induced dilations in metallic glasses. *Scripta Met.*, 19, pp. 591-596.

Aronin, A. S. (2001). Formation and structure of nanocrystals in an $Al_{86}Ni_{11}Yb_3$ metallic glass. *Physics of the Solid State*, 43, 1, pp. 2003-2011.

Bae, D. H., Lee, M. H., Kim, D. H., &Sordelet, D. J. (2003). Plasticity in Ni59Zr20Ti16Si 2Sn3 metallic glass matrix composites containing brass fibers synthesized by warm extrusion of powders. *Applied Physics Letters*, 83, 12, pp. 2312-2314.

Battezzati, L., &Baldissin, D. (2008). Quantitative evaluation of lengthscales for temperature rise in shear bands and for failure of metallic glasses. *Scripta Materialia*, 59, 2, pp. 223-226.

Bian, Z., He, G., &Chen, G. L. (2002). Investigation of shear bands under compressive testing for Zr-base bulk metallic glasses containing nanocrystals. *Scripta Materialia*, 46, 6, pp. 407-412.

Boswell, P. G. (1979). Wear resistance of liquid quenched metallic glass. *Journal of Materials science*, 14, pp. 1505-1507.

Cahn, J.W. (1961). On spinodal decomposition, Acta Metall., 9, pp. 795-801

Calvayrac, Y., Harmelin, M., Quivy, A., Chevalier, J. P., &Bigot, J. (1980). COLD-ROLLING AND SUBSEQUENT ANNEALING OF AMORPHOUS Cu60Zr40. *Scripta metallurgica*, 14, 8, pp. 895-898.

Chen, H., He, Y., Shiflet, G. J., &Poon, S. J. (1994). Deformation-induced nanocrystal formation in shear bands of amorphous alloys. *Nature*, 367, 6463, pp. 541-543.

Christian, J.W. (1975). The theory of transformations in metals and alloys, Pergamon.

Claus, J. C., &von Heimendahl, M. (1983). Influence of superimposed tensile stress on metallic glass crystallization. *Zeitschrift fur Metallkunde*, 74, 11, pp. 744-750.

Csontos, A. A., &Shiflet, G. J. (1997). Composition profiles associated with nanocrystal formation in aluminum-rich metallic glasses, Orlando, FL, USA, TMS.

Dandliker, R. B., Conner, R. D., &Johnson, W. L. (1998). Melt infiltration casting of bulk metallic-glass matrix composites. *Journal of Materials Research*, 13, 10, pp. 2896-2901.

Donovan, P. E., &Stobbs, W. M. (1983). Shear band interactions with crystals in partially crystallised metallic glasses. *Journal of Non-Crystalline Solids*, 55, 1, pp. 61-76.

Duwez, P. (1981). Metallic glasses - historical background. Glassy Metals I. H.-J. Guentherodt and H. Beck. Berlin Heidelberg New-York, Springer-Verlag. I: 19-23.

Emmens, W.C., Vrijen, J., &Radelaar, S. (1975). Crystallization of amorphous $Pd_{0.75}Ag_{0.05}Si_{0.2}$ under hydrostatic stress. *J. Non-Cryst. Solids*, 18, pp. 299-302.

Freestone, I., Meeks, N., Sax, M., &Higgitt, C. (2007). The Lycurgus Cup - A Roman Nanotechnology. *Gold Bulletin*, 40, 4, pp. 270-276.

Glicksman, M.E. (2000). Diffusion in solids, John Wiley & Sons, Inc.

Gloriant, T. (2003). Microhardness and abrasive wear resistance of metallic glasses and nanostructured composite materials. *Journal of Non-Crystalline Solids*, 316, pp. 96-103.

Gloriant, T., &Greer, A. L. (1998). Al-based nanocrystalline composites by rapid solidification of Al-Ni-Sm alloys. *NanoStruct. Mater.*, 10, 3, pp. 389-396.

Gloriant, T., Ping, D.H., Hono, K., Greer, A.L., &Baro, M.D. (2001). Nanostructured Al88Ni4Sm8 alloys investigated by transmission electron and field-ion microscopies. *Mater. Sci. Engr. A*, A304-306, pp. 315-320.

Greer, A. L. (1995). Metallic Glasses. *Science*, 267, pp. 1947-1953.

Greer, A. L., Rutherford, K. L., &Hutchings, I. M. (2002). Wear resistance of amorphous alloys and related materials. *International Materials Reviews*, 47, 2, pp. 87-112.

Greer, A. L., Rutherford, K. L., &Hutchings, M. (2002). Wear resistance of amorphous alloys and related materials. *International Materials Reviews*, 47, 2, pp. 87-112.

Gryaznov, V. G., Polonsky, I. A., Romanov, A. E., &Trusov, L. I. (1991). Size effects of dislocation stability in nanocrystals. *Physical Review B (Condensed Matter)*, 44, 1, pp. 42-46.

Gu, X. J., Poon, S. J., Shiflet, G. J., &Widom, M. (2008). Ductility improvement of amorphous steels: roles of shear modulus and electronic structure. *Acta Materialia*, 56, 1, pp. 88-94.

Hashimoto, K. (2002). In pursuit of new corrosion-resistant alloys. *Corrosion*, 58, pp. 715.

Hays, C. C., Kim, C. P., &Johnson, W. L. (2000). Microstructure controlled shear band pattern formation and enhanced plasticity of bulk metallic glasses containing in situ formed ductile phase dendrite dispersions. *Physical Review Letters*, 84, 13, pp. 2901-2904.

Hebert, R. J., Boucharat, N., Perepezko, J. H., Rosner, H., &Wilde, G. (2005). Deformation-induced crystallization reactions in amorphous $Al_{88}Y_7Fe_5$ alloy, Phoenix, AZ, United States, Minerals, Metals and Materials Society, Warrendale, PA 15086, United States.

Hebert, R. J., &Perepezko, J. H. (2004). Effect of cold-rolling on the crystallization behavior of amorphous $Al_{88}Y_7Fe_5$ alloy, Oxford, UK, Elsevier.

Hebert, R. J., Perepezko, J. H., Rosner, H., &Wilde, G. (2006). Dislocation formation during deformation-induced synthesis of nanocrystals in amorphous and partially crystalline amorphous Al88Y7Fe5 alloy. *Scripta Materialia*, 54, 1, pp. 25-29.

Hebert, R.J., &Perepezko, J. H. (2007). Driven nanocrystal catalysis for amorphous Al-Y-Fe alloys. *Met. Trans. A*, to be published, pp.

Hebert, Rainer J., Rosner, Harald, Wilde, Gerhard, &Perepezko, John H. (2004). Deformation-induced devitrification of Al-based amorphous alloys. *JOM*, 56, 11, pp. 269.

Hillert, M. (1968). The role of interfaces in phase transformations. The mechanism of phase transformations in crystalline solids, Manchester, The Institute of Metals, London.

Hongwen, Zhang, Subhash, G., &Maiti, S. (2007). Local heating and viscosity drop during shear band evolution in bulk metallic glasses under quasistatic loading. *Journal of Applied Physics*, 102, 4, pp. 043519-043511.

Hono, K., Zhang, Y., Tsai, A.P., Inoue, A., &Sakurai, T. (1995). Solute partitioning in partially crystallized Al-Ni-Ce(-Cu) metallic glasses. *Scripta Met. Mat.*, 32, 2, pp. 191-196.

Inoue, A. (1998). Amorphous, nanoquasicrystalline and nanocrystalline alloys in Al-based systems. *Progr. Mater. Sci.*, 43, pp. 365-.

Iwasaki, H., &Masumoto, T. (1978). Effect of high pressure on the crystallization of an amorphous $Pd_{80}Si_{20}$ alloy. *J. Mater. Sci.*, 13, pp. 2171-2176.

Jiang, W. H., &Atzmon, M. (2003). The effect of compression and tension on shear-band structure and nanocrystallization in amorphous $Al_{90}Fe_5Gd_5$: A high-resolution transmission electron microscopy study. *Acta Materialia*, 51, 14, pp. 4095-4105.

Jiang, W. H., Liu, F. X., Liao, H. H., Choo, H., Liaw, P. K., Edwards, B. J., &Khomami, B. (2008). Temperature increases caused by shear banding in as-cast and relaxed Zr-based bulk metallic glasses under compression. *Journal of Materials Research*, 23, 11, pp. 2967-2974.

Jiang, W. H., Liu, F. X., Liaw, P. K., &Choo, H. (2007). Shear strain in a shear band of a bulk-metallic glass in compression. *Applied Physics Letters*, 90, 18, pp.

Jiang, W. H., Pinkerton, F. E., &Atzmon, M. (2003). Effect of strain rate on the formation of nanocrystallites in an Al-based amorphous alloy during nanoindentation. *Journal of Applied Physics*, 93, 11, pp. 9287-9290.

Jin, H. J., Zhou, F., Wang, L. B., &Lu, K. (2001). Effect of plastic deformation on thermal stability in metallic glasses. *Scripta Materialia*, 44, 7, pp. 1083-1087.

Kim, D. H., Chang, H. J., Kim, Y. M., Kim, Y. J., &Chattopadhyay, K. (2006). On the origin of nanocrystals in the shear band in a quasicrystal forming bulk metallic glass Ti40Zr29Cu9Ni8Be14. *Scripta Materialia*, 55, 6, pp. 509-512.

Kim, J. J., Choi, Y., Suresh, S., &Argon, A. S. (2002). Nanocrystallization during nanoindentation of a bulk amorphous metal alloy at room temperature. *Science*, 295, 5555, pp. 654-657.

Kingery, W.D., Bowen, H.K., &Uhlmann, D.R. (1976). Introduction to ceramics, John Wiley & Sons, Inc.

Kishore, Sudarsan, U., Chandran, N., &Chattopadhyay, K. (1987). On the wear mechanism of iron and nickel based transition metal-metalloid metallic glasses. *Acta Metallurgica*, 35, 7, pp. 1463-1473.

Klinger, R., &Feller, H. G. (1983). Sliding friction and wear resistance of the metallic glass $Fe_{40+}Ni_{40}B_{20}$ *Wear*, 86, pp. 287-297.

Koch, C. C. (1989). Materials synthesis by mechanical alloying. Annual review of material science. Vol.19. Palo Alto, CA, USA, Annual Reviews: 121-143.

Koester, U. (1993). Phase transformations in rapidly solidified alloys. *Key Engr. Mat.*, 81-83, pp. 647-662.

Kulik, T., &Matyja, H. (1980). The effect of plastic deformation of amorphous Pd-Si alloys on their thermal properties. *Journal of Materials Science*, 15, 12, pp. 3169-3172.

Lee, Seok-Woo, Huh, Moo-Young, Chae, Soo-Won, &Lee, Jae-Chul (2006). Mechanism of the deformation-induced nanocrystallization in a Cu-based bulk amorphous alloy under uniaxial compression. *Scripta Materialia*, 54, 8, pp. 1439-1444.

Lewandowski, J. J., &Greer, A. L. (2006). Temperature rise at shear bands in metallic glasses. *Nature Materials*, 5, 1, pp. 15-18.

Li, G., Wang, Y. Q., Wang, L. M., Gao, Y. P., Zhang, R. J., Zhan, Z. J., Sun, L. L., Zhang, J., &Wang, W. K. (2002). Wear behavior of bulk Zr41Ti14Cu12.5Ni10Be22.5 metallic glasses. *Journal of Materials Research*, 17, 8, pp. 1877-1880.

Lim, S.C., &Ashby, M.F. (1987). Overview No. 55 Wear mechanism maps. *Acta Metallurgica*, 35, 1, pp. 1-24.

Liu, X. J., Chen, G. L., Hui, X. D., Hou, H. Y., Yao, K. F., &Liu, C. T. (2007). Growth mechanism from nano-ordered clusters to nanocrystals in a deeply undercooled melt of Zr-Ni-Ti metallic glass. *Journal of Applied Physics*, 102, 6, pp.

Louzguine-Luzgin, D. V., &Inoue, A. (2006). Comparative study of the effect of cold rolling on the structure of Al-RE-Ni-Co (RE=rare-earth metals) amorphous and glassy alloys. *Journal of Non-Crystalline Solids*, 352, 36-37, pp. 3903-3909.

Louzguine-Luzgin, D. V., &Inoue, A. (2006). Observation of linear defects in Al particles below 7 nm in size. *Journal of Materials Research*, 21, 6, pp. 1347-1350.

Louzguine-Luzgin, D. V., &Inoue, A. (2007). Investigation of a rapidly solidified Al-based nanocomposite with extremely high number density of precipitates. *Materials*

Science & Engineering A (Structural Materials: Properties, Microstructure and Processing), 449-451, pp. 1026-1028.

Luborsky, F. E., Walter, J. R., &LeGrand, D. G. (1976). Cold-rolling and annealing of amorphous ribbons, USA.

Lucente, A., &Scully, J. R. (2008). Localized corrosion of Al-based amorphous-nanocrystalline alloys with solute-lean nanocrystals: pit stabilization. *J. Electrochem. Soc.*, 155, 5, pp. C234-C243.

Maddala, D., &Hebert, R.J. (2011). Effect of notch toughness and hardness on sliding wear of Cu50Hf41.5Al8.5 bulk metallic glass. *Scripta Mater., submitted*, pp.

Maddala, D., Mubarok, A., &Hebert, R.J. (2010). Sliding wear behavior of Cu50Hf41.5Al8.5 bulk metallic glass. *Wear*, 269, 7-8, pp. 572-580.

Maddin, R., &Masumoto, T. (1972). The deformation of amorphous palladium-20 at.% silicon. *Material Science and Engineering*, 9, 3, pp. 153-162.

Masumoto, T., &Maddin, R. (1975). Structural stability and mechanical properties of amorphous metals. *Material Science and Engineering*, 19, 1, pp. 1-24.

Miyoshi, Kazuhisa, &Buckley, Donald H. (1983). Friction and wear of some ferrous-base metallic glasses, Lewis Res. Cent.,Natl. Aeronaut. Space Adm.,Cleveland,OH,USA.: 24 pp.

Miyoshi, Kazuhisa, &Buckley, Donald H. (1983). Sliding-induced crystallization of metallic glass, Lewis Res. Cent.,Natl. Aeronaut. Space Adm.,Cleveland,OH,USA.: 23 pp.

Miyoshi, Kazuhisa, &Buckley, Donald H. (1984). Friction and wear of some ferrous-base metallic glasses. *ASLE Transactions*, 27, 4, pp. 295-304.

Mubarok, A., &Hebert, R.J. The Kauzmann temperature of a Ce69.5Al10Cu20Co0.5 bulk metallic glass based on calorimetric and volumetric analyses. *in preparation*, pp.

Mullins, W.W., &Sekerka, R.F. (1963). Morphological stability of a particle growing by diffusion or heat flow. *J. Appl. Phys.*, 34, 2, pp. 323-329.

Noskova, N. I., Vil'danova, N. F., Tagirov, R. I., Potapov, A. P., &Glazer, A. A. (1989). Influence of rolling reduction on the crystallization process of amorphous alloy $Fe_{81}Si_7B_{12}$ *Phys. Met. Metall.*, 67, 6, pp. 136-143.

Ogura, A., Tarumi, R., Shimojo, M., Takashima, K., &Higo, Y. (2001). Control of nanocrystalline orientation using application of a stress field in an amorphous alloy. *Appl. Phys. Lett.*, 79, 7, pp. 1042-1044.

Ott, R. T., Sansoz, F., Molinari, J. F., Almer, J., Ramesh, K. T., &Hufnagel, T. C. (2005). Micromechanics of deformation of metallic-glass-matrix composites from in situ synchrotron strain measurements and finite element modeling. *Acta Materialia*, 53, 7, pp. 1883-1893.

Paillier, J., Mickel, C., Gostin, P.F., Gebert, A. (2010). Characterization of corrosion phenomena of Zr-Ti-Cu-Al-Ni metallic glass by SEM and TEM, Mater. Charact., 61, pp. 1000-1008.

Park, J. S., Lim, H. K., Kim, J. H., Chang, H. J., Kim, W. T., Kim, D. H., &Fleury, E. (2005). In situ crystallization and enhanced mechanical properties of the Zr41.2Ti13.8Cu12.5Ni10Be22.5 alloy by cold rolling. *Journal of Non-Crystalline Solids*, 351, 24-26, pp. 2142-2146.

Patterson, J., &Jones, D.R.H. (1979). The effect of homogeneous deformation on the crystallization of a metallic glass. *Scripta Met.*, 13, pp. 947-949.

Perepezko, J. H., &Hebert, R. J. (2002). Amorphous aluminum alloys - synthesis and stability. *JOM*, 54, 3, pp. 34-39.

Perepezko, J. H., Imhoff, S. D., &Hebert, R. J. (2010). Nanostructure development during devitrification and deformation. *Journal of Alloys and Compounds*, 495, 2, pp. 360-364.

Purdy, G.R. (1981). Interface diffusion-controlled kinetics and mechanisms. Int. Conf. on solid-solid phase transformations, Pittsburgh, The Metallurgical Society AIME.

Ratke, L., &Vorhees, P.W. (2001). Growth and Coarsening, Springer.

Sadoc, Anne, Heckmann, Olivier, Nassif, Vivian, Proux, Olivier, Hazemann, Jean-Louis, Xing, L. Q., &Kelton, K. F. (2007). Local order and nanostructure induced by microalloying in Al-Y-Fe amorphous alloys. *Journal of Non-Crystalline Solids*, 353, 29, pp. 2758-2766.

Schroers, Jan, &Johnson, William L. (2004). Ductile bulk metallic glass. *Physical Review Letters*, 93, 25, pp. 255506-255501-255506-255504.

Schuh, C. A., Hufnagel, T. C., &Ramamurty, U. (2007). Overview No.144 - Mechanical behavior of amorphous alloys. *Acta Materialia*, 55, 12, pp. 4067-4109.

Schulz, R., Trudeau, M. L., Dussault, D., &Van Neste, A. (1990). Crystallization of amorphous alloys by high energy mechanical deformation. *Colloque de Physique C4*, 51, Suppl. No.14, pp. C-4 259 - C-254 264.

Schulz, R., Trudeau, M. L., Dussault, D., &Van Neste, A. (1990). Crystallization of amorphous alloys by high energy mechanical deformation, France.

Scully, J. R., Gebert, A., &Payer, J. H. (2007). Corrosion and related mechanical properties of bulk metallic glasses. *Journal of Materials Research*, 22, 2, pp. 302-313.

Scully, J. R., &Lucente, A. (2005). Corrosion of amorphous metals. *Met. Mat. Trans. B*, 13B, pp. 476.

Sharma, S.K., &Banerjee, S. (1989). Some correlations for diffusion in amorphous alloys. *J. Mater. Res.*, 4, 3, pp. 603-606.

Spaepen, Frans, &Turnbull, David (1974). Mechanism for the flow and fracture of metallic glasses. *Scripta Metallurgica*, 8, 5, pp. 563-568.

Stratton, W. G., Hamann, J., Perepezko, J. H., Voyles, P. M., Mao, X., &Khare, S. V. (2005). Aluminum nanoscale order in amorphous Al92Sm8 measured by fluctuation electron microscopy. *Applied Physics Letters*, 86, 14, pp. 141910-141913.

Suryanarayana, C., &Inoue, A. (2011). Effect of pressure during annealing. Bulk Metallic Glasses, CRC Press: 250-254.

Tam, C. Y., &Shek, C. H. (2004). Abrasive wear of Cu60Zr30Ti10 bulk metallic glass. *Materials Science and Engineering a-Structural Materials Properties Microstructure and Processing*, 384, 1-2, pp. 138-142.

Tarumi, Ryuichi, Ogura, Akio, Shimojo, Masayuki, Takashima, Kazuki, &Higo, Yakichi (2000). Molecular dynamics simulation of crystallization in an amorphous metal during shear deformation. *Japanese Journal of Applied Physics, Part 2: Letters*, 39, 6 B, pp. 611-613.

Tiwari, R. S., Claus, J. C., &von Heimendahl, M. (1982). The effect of tensile stress on the crystallization kinetics of Metglas 2826 $Fe_{40}Ni_{40}P_{14}B_6$. *Material Science and Engineering*, 55, 1, pp. 1-7.

Vom Wege, F., Kumpfert, J., &Hornbogen, E. (1991). Mikrokratzertests an einer schmelzgesponnenen und nachfolgend angelassenen Co-Basislegierung. *Z. Metallkde.*, 82, pp. 209-216.

Vom Wege, F., Skrotzki, B., &Hornbogen, E. (1988). Abrasivverschleiss einer schmelzgesponnenen und nachfolgend angelassenen Co-Basis Legierung. *Z. Metallkde.*, 79, pp. 492-498.

Yeong-Hwan, Kim, Inoue, A., &Masumoto, T. (1991). Ultrahigh mechanical strengths of $Al_{88}Y_2Ni_{10-x}M_x$ (M=Mn, Fe or Co) amorphous alloys containing nanoscale FCC-Al particles. *Materials Transactions, JIM*, 32, 7, pp. 599-608.

Zener, C. (1949). Theory of growth of spherical precipitates from solid solution. *J. Appl. Phys.*, 20, pp. 950-953.

Zhang, Y., Hono, K., Inoue, A., Makino, A., &Sakurai, T. (1996). Nanocrystalline structural evolution in Fe90Zr7B3 soft magnetic material. *Acta Mat.*, 44, 4, pp. 1497-1510.

Zhang, Y., Warren, P.J., &Cerezo, A. (2002). Effect of Cu addition on nanocrystallization of Al-Ni-Sm amorphous alloy. *Mater. Sci. Engr. A*, A327, pp. 109-115.

Zum Gahr, K.H., &Noecker, H. (1981). Abrasivverschleiss metallischer Glaeser. *Metall*, 35, 10, pp. 988-995.

Paillier, J., Mickel, C., Gostin, P.F., Gebert, A. (2010). Characterization of corrosion phenomena of Zr-Ti-Cu-Al-Ni metallic glass by SEM and TEM, *Mater. Charact.,* 61, pp. 1000-1008.

Ye, F., &Lu, K. (1999) Pressure effect on crystallization kinetics of an Al-La-Ni amorphous alloy, Acta Mater., 47,8, pp. 2449-2454

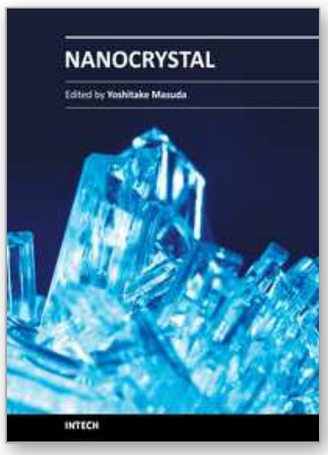

Nanocrystal

Edited by Dr. Yoshitake Masuda

ISBN 978-953-307-199-2
Hard cover, 494 pages
Publisher InTech
Published online 28, June, 2011
Published in print edition June, 2011

We focused on cutting-edge science and technology of Nanocrystals in this book. â€œNanocrystalâ€ is expected to lead to the creation of new materials with revolutionary properties and functions. It will open up fresh possibilities for the solution to the environmental problems and energy problems. We wish that this book contributes to bequeath a beautiful environment and valuable resources to subsequent generations.

How to reference

In order to correctly reference this scholarly work, feel free to copy and paste the following:

Rainer J. Hebert (2011). Nanocrystals in Metallic Glasses, Nanocrystal, Dr. Yoshitake Masuda (Ed.), ISBN: 978-953-307-199-2, InTech, Available from: http://www.intechopen.com/books/nanocrystal/nanocrystals-in-metallic-glasses

INTECH
open science | open minds

InTech Europe
University Campus STeP Ri
Slavka Krautzeka 83/A
51000 Rijeka, Croatia
Phone: +385 (51) 770 447
Fax: +385 (51) 686 166
www.intechopen.com

InTech China
Unit 405, Office Block, Hotel Equatorial Shanghai
No.65, Yan An Road (West), Shanghai, 200040, China
中国上海市延安西路65号上海国际贵都大饭店办公楼405单元
Phone: +86-21-62489820
Fax: +86-21-62489821

IntechOpen